Gene Therapy (2012) 19, 176–181

www.nature.com/gt

SHORT COMMUNICATION

Enhanced gene delivery to the neonatal retina through systemic administration of tyrosine-mutated AAV9

D Dalkara[1,2], LC Byrne[3], T Lee[3], NV Hoffmann[3], DV Schaffer[1,2] and JG Flannery[3]

Delivery of therapeutic genes to a large region of the retina with minimal damage from intraocular surgery is a central goal of treatment for retinal degenerations. Recent studies have shown that AAV9 can reach the central nervous system (CNS) and retina when administered systemically to neonates, which is a promising strategy for some retinal diseases. We investigated whether the retinal transduction efficiency of systemically delivered AAV9 could be improved by mutating capsid surface tyrosines, previously shown to increase the infectivity of several AAV vectors. Specifically, we evaluated retinal transduction following neonatal intravascular administration of AAV9 vectors containing tyrosine to phenylalanine mutations at two highly conserved sites. Our results show that a novel, double tyrosine mutant of AAV9 significantly enhanced gene delivery to the CNS and retina, and that gene expression can be restricted to rod photoreceptor cells by incorporating a rhodopsin promoter. This approach provides a new methodology for the development of retinal gene therapies or creation of animal models of neurodegenerative disease.
Gene Therapy (2012) **19,** 176–181; doi:10.1038/gt.2011.163; published online 20 October 2011

Keywords: Adeno-associated virus; systemic; retina; animal models of neurodegenerative disease

INTRODUCTION

Numerous retinal degenerative diseases are caused by single gene mutations that lead to either loss of protein function or gain of deleterious properties. Recently, adeno-associated viral vector-mediated gene therapy has been successful in three separate clinical trials for treating the monogenic retinal dystrophy LCA2 caused by mutations in the retinoid isomerase retinal pigment epithelium (RPE)65.[1–3] These clinical trials clearly demonstrate that AAV-mediated gene replacement therapies are an effective strategy for treating inherited retinal degeneration. In addition, they demonstrate proof of concept for ocular gene therapy, which hopefully can be extended to treat dominant disease involving gain of function mutations via the delivery of gene constructs that induce RNA interference.

Reviewing the positive LCA2 results underscores the importance of the surgical route of delivery to successful treatment outcome. The vast majority of retinal disease mutations affect photoreceptors and the RPE.[4] Vector administration into the subretinal space, in close proximity with these cells, has been preferable for gene replacement strategies targeting the outer retina. This approach is highly effective at generating localized expression of the transgene at levels sufficient to correct the retinal degeneration phenotype in LCA2[5] or where a diffusible factor is secreted from a group of infected cells in sufficient quantities to benefit the whole tissue.[6] However, subretinal injections are highly invasive and induce a transient retinal detachment, which is damaging to the photoreceptors.

An ideal approach to address retinal dystrophies that affect large areas of the retina would be to deliver the viral vector into the vitreous cavity. Unfortunately, there are a number of formidable barriers impeding gene delivery to the retina from the vitreous such as diffusion in the vitreous cavity and sequestering of viral particles in the inner limiting membrane. Although much progress has been made in the understanding of barriers to retinal transduction from the vitreous for AAV[7,8] as well as improving the limited transduction of the naturally occurring serotypes by rational[9,10] and directed evolution approaches[11,12] major obstacles remain in reaching therapeutically effective levels of gene expression, especially in larger animals where the inner limiting membrane is significantly thicker than in rodents.[13]

An alternative approach for transducing large areas of retina is to administer vectors through the ocular vasculature. The retina is a highly vascularized structure with the highest oxygen consumption per weight of any human tissue.[14] The retina is nourished by a dual blood supply from the choroidal capillaries (supplying the outer retina) and by branches of the central retinal artery (supplying two thirds of the inner neural retina) (Figure 1). Vectors that can penetrate the blood–retinal barrier have the potential to access both inner and outer retinal layers. Although administration of gene delivery vehicles from the vasculature entails greater immunological risks,[15] it may be particularly promising in neonates where the immaturity of the newborn immune system leads to a 'physiological immunodeficiency' that encompasses all arms of the host response.

It was recently demonstrated that the retina can be transduced via neo-natal systemic administration of AAV,[16] though the utility of this seminal study has been somewhat limited to date by the relatively low levels of gene expression observed in limited retinal cell types, potentially because of the relatively low dosages used. Importantly, recent reports have shown that the central nervous system can be very

[1]Department of Chemical Engineering, The Helen Wills Neuroscience Institute, The University of California, Berkeley, CA, USA; [2]Department of Bioengineering, The Helen Wills Neuroscience Institute, The University of California, Berkeley, CA, USA and [3]Department of Molecular and Cellular Biology, The Helen Wills Neuroscience Institute, The University of California, Berkeley, CA, USA
Correspondence: Dr D Dalkara, Department of Chemical Engineering, and The Helen Wills Neuroscience Institute, University of California Berkeley, 132 Barker Hall, Berkeley, CA 94720-3190, USA.
E-mail: deniz.dalkara@gmail.com
Received 5 August 2011; revised 14 September 2011; accepted 19 September 2011; published online 20 October 2011

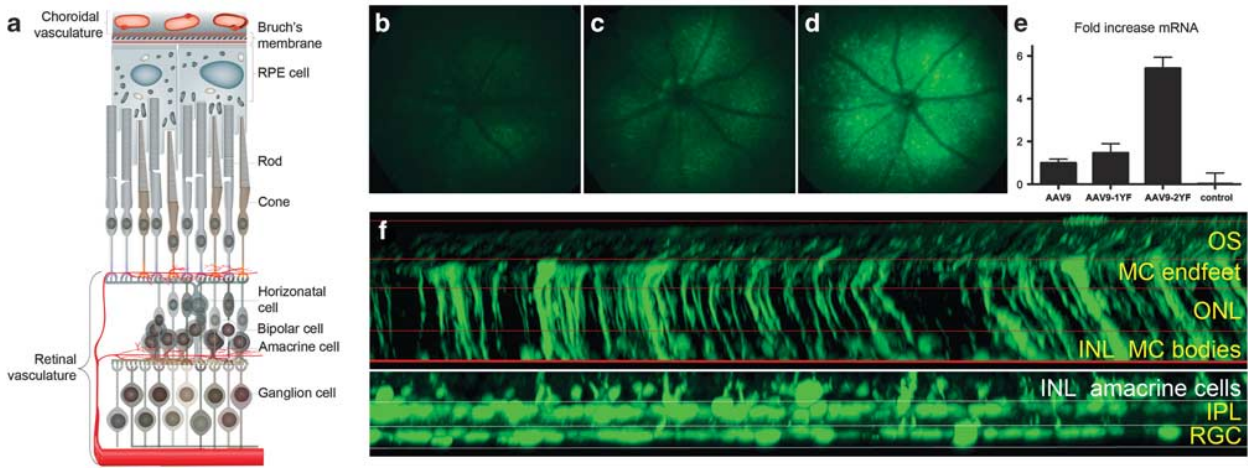

Figure 1 (**a**) Illustration depicting the dual blood supply of the retina. The inner two thirds of the retina is perfused by capillary networks of the central retinal artery, whereas the outer third receives its blood supply from the choroidal vasculature. The choroidal circulation has a higher flow rate and a fenestrated (leaky) capillary bed. (**b–d)** Quantitative comparison of AAV9, AAV9-1YF and AAV9-2YF. Representative fundus photographs showing GFP expression in live mice that received tail vein injections of (**a**) AAV9, (**b**) AAV9-1YF or (**c**) AAV9-2YF 1 month after injection. Visible fluorescence using fundus imaging was detectable in eyes 2 weeks post-injection and stayed constant after that time point. (**e**) RNA extracted from retinas of AAV9 (n=5), AAV9-1YF (n=4) or AAV9-2YF (n=5) injected mice retinas were pooled, and RT-PCR was performed in triplicate. The ddCT method was used to calculate fold difference of GFP expression normalized to AAV9. Error bars depict the s.d.s of dCT values. An uninjected mouse retina was included as a negative control. (**f**) 3D reconstruction of a representative retinal flatmount showing transduction with AAV9-2YF. Scanning confocal micrographs were acquired with 0.84 μm intervals through the inner and outer retinas transduced with AAV9-2YF using a ×20 objective. The lower image was collected from a retinal flatmount lying with the RGC side facing upwards. The upper image was collected from the contralateral retina mounted with the photoreceptor side facing up to avoid reduction of signal in the deeper layers of the tissue. Stacks were assembled to provide 3D reconstruction using IMARIS software (Bitplane Inc., Windsor, CT, USA). INL, inner nuclear layer; IPL, inner plexiform layer; MC, Müller cell; ONL, outer nuclear layer; OS, outer segment.

effectively transduced via systemic administration[17–19] and the higher doses and use of self-complimentary vector genomes in these studies[20] may have contributed to this capability. These results suggest that improving the vector delivery system holds promise for enhancing retinal transduction while limiting the number of viral particles necessary to achieve sufficient levels of protein expression.

The AAV capsid is a critical determinant of vector transduction efficiency, mediating vector binding to cell surface receptors, internalization, cytoplasmic trafficking to the nuclear membrane and vector genome release.[21] It has been shown that tyrosines exposed on the AAV capsid surface can undergo tyrosine kinase-mediated phosphorylation, leading to ubiquitination and degradation of viral particles. Site-directed tyrosine to phenylalanine (Y-F) mutagenesis of one or more of the seven capsid surface-exposed AAV tyrosine residues in the VP3 common region has been reported to protect vector particles from proteasome degradation and yield significant increases in the transduction efficiency of mutant vectors relative to their wild-type counterparts.[9,22] For example, AAV2, AAV8 or AAV9 vectors containing single Y-F point mutations on two of the seven surface-exposed capsid tyrosine residues are significantly more efficient at transduction of retinal cells when injected subretinally or intravitreally.[9]

Here, we investigate whether retinal transduction via intravenous delivery to neonatal mice is enhanced by using AAV9 vector variants containing single or double Y-F mutations. We report that our double tyrosine mutant exhibits robust transgene expression in all retinal layers following a single intravascular injection in neonates. The potential to transduce photoreceptors and RPE cells (the targets of most inherited retinal degenerations)—as well as ganglion cells, amacrine cells and Müller glia—following systemic vector delivery represents a promising alternative to surgically traumatic subretinal injections that are currently necessary to transduce these cell types and opens new avenues in experimental gene therapy. Furthermore, the ability to efficiently target the photoreceptor and RPE cells of the retina bilaterally suggests this technology can be used to generate primate animal models of retinal degeneration.[23] For example, a novel transgenesis approach based not on germ line transgenesis, but instead harnessing AAV vectors to overexpress causative, mutant RP genes in the photoreceptors of models such as the macaque, could offer an attractive strategy to generate primate models of retinal degeneration.[24]

RESULTS AND DISCUSSION

Quantitative and histological comparison of AAV9, AAV9-1YF vs AAV9-2YF-mediated green fluorescent protein (GFP) expression

Single phenylalanine (F) to tyrosine (Y) substitutions at positions 446 or 731 have been shown to increase retinal transduction by AAV9 following intraocular administration.[9] On the basis of these findings, we introduced a single tyrosine mutation at position 446 of AAV9 either alone (AAV9-1YF) or in combination with additional mutation at position 731 (AAV9-2YF).

Histology, fundus imaging and reverse transcriptase (RT)-PCR were used to quantify levels of GFP expression resulting from AAV9 and its tyrosine-mutated variants. Retinal flatmounts from pups 1 week post injection exhibited strong GFP expression in the retinal ganglion cells (RGC) (Supplementary Figure 1), indicating a very early onset of gene expression. Two weeks after injection, at eyelid opening in pups, fundus imaging was performed, and the highest levels of GFP fluorescence were detected with AAV9-2YF (Figures 1b–d). AAV9-1YF showed lower levels of GFP expression compared with AAV9-2YF but higher than AAV9 (Figure 1c). We evaluated the amounts of GFP expression in a more quantitative fashion, by performing RT-PCR on pooled RNA extracted from retinal lysates obtained from pups injected with each of the viruses (n=5 for AAV9, n=4 AAV9-1YF

and n=5 for AAV9-2YF). RT-PCR results indicated a sixfold improvement for AAV9-2YF over AAV9 (Figure 1e).

Following these observed enhancements in GFP expression using the mutant AAV9 capsids, we evaluated the histological expression patterns of GFP in the retinal layers via confocal microscopy 8 weeks after injection. In agreement with the fundus images, the retinas that received AAV9-2YF exhibited an average of 3.3-fold more GFP in all retinal layers excluding the RPE (Supplementary Figures 1b and c). Confocal z-stacks spanning the entire length of the retina showed GFP expression in all retinal layers for AAV9-2YF, as depicted in a 3D reconstruction side view (Figure 1f).

GFP expression obtained with AAV9 was compared with its tyrosine-mutated counterparts; to do so the microscope was adjusted to the fluorescence intensity using the AAV9-2YF retina, and the same settings were retained for all subsequent acquisitions at each of the retinal layers. For each image, a ×10 objective was used to image 212×212 μm fields next to the optic nerve head. Confocal z-stacks spanning 5–15 μm of the RGC layer, inner nuclear layer, photoreceptor layer, and RPE cells were acquired and merged (Figures 2a–l). Our results consistently show that GFP expression is stronger with AAV9-2YF in each layer (see Supplementary Figures 2b and c for quantification of the GFP intensity in each layer). The most striking differences between the wild-type AAV9 and AAV9-2YF are observed in the number of transduced inner retinal cells and photoreceptor cells (Figures 2a–i). In 212×212 μm regions of the retinas close to the optic nerve head represented in Figure 2, we found 112 GFP (+) cells in the RGC layer with AAV9 compared with 344 using AAV9-2YF. In the inner nuclear layer there were 222 GFP (+) cells for AAV9 and 606 for AAV9-2YF. A total of 218 GFP (+) photoreceptors were found using AAV9 compared with 823 with AAV9-2YF.

All vectors lead to significant levels of expression in the RPE and RGC cells (Figures 2 and 3). Interestingly, however, an insignificant number of bipolar cells were transduced with AAV9-2YF or other capsid variants (Figures 3g–i). Higher magnification images of the AAV-2YF-treated retinas further reveal transgene expression in the RGC layer (Figure 3j, with NeuN staining in red), the inner nuclear layer (Figure 3k) and the outer nuclear layer (Figure 3l). Additional, histological examination of the transduced retinas reveals striking differences, notably in the transduction of inner nuclear layer and photoreceptor cells (Figures 3a–i). These observations correlate with the anatomical and physiological features of the retinal blood supply (Figure 1a). That is, fenestrated choroidal vessels perfuse the outer retina and provide vector access to the basolateral RPE, whereas, arteries and veins lying within the nerve fiber layer give rise to fine capillaries that perfuse the inner retina. Thus, a gradient of GFP expression could result from AAV transport into the retina from the inner and outer blood supplies, with the RPE and ganglion cells closest to the initial sources of vector. As predicted by the anatomy, we observe the strongest transduction in the inner and outermost layers of the retina with the wild-type AAV9 virus. Introduction of tyrosine mutations enables more efficient transduction of the middle retina, which previously had undetectable levels of expression with the wild-type AAV9.

Expression in the mouse brain using AAV9 and its tyrosine-mutated counterparts

The enhanced retinal transduction by AAV9-2YF compared with wild-type AAV9 led us to examine transduction of various brain regions. Analogous increases in transduction levels were observed with AAV9-2YF (left column) compared with AAV9 (right column) in all brain regions examined (Figures 4a–h, Supplementary Figure 3).

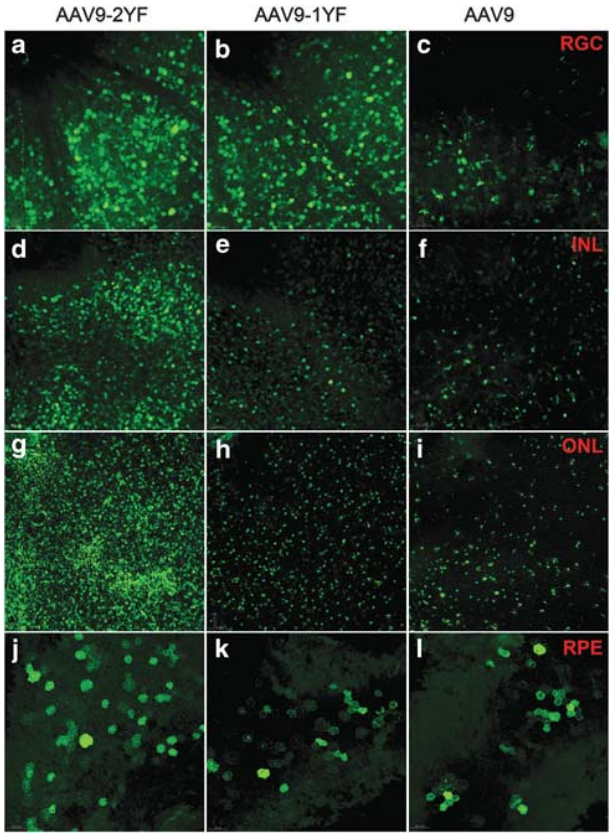

Figure 2 Empirical comparison of AAV9, AAV9-1YF and AAV9-2YF (**a–l**) Z-projections of confocal stacks acquired from representative retinas transduced with AAV9, AAV9-1YF or AAV9-2YF. Representative retinas were harvested and dissected to separate the retinal tissue from its underlying choroid and RPE cells. The retinas were mounted flat on one side, and the corresponding choroid with the detached RPE cells was mounted separately. The confocal stacks were taken close to the optic nerve head at different depths from the retinal surface, scanning one retinal cell layer at a time. The optic nerve appears on the upper left hand corner of each image. Expression in the RGC layer is shown for each virus, including (**a**) AAV9-2YF in the left column, (**b**) AAV9-1YF in the middle column and (**c**) AAV9 in the right column. The second row (**d–f**) shows expression at the inner nuclear layer cell bodies with the same viruses. (**g–i**) Correspond to GFP fluorescence from cell bodies in the photoreceptor layer. The last row (**j–l**) shows a z-projection image collected from the RPE flatmounts corresponding to the retinas. All stacks were acquired using identical acquisition parameters. The acquisition parameters were initially tuned for retinas transduced with AAV9-2YF, then used for all retinas.

Consistent with previous reports for AAV9, GFP-positive cells included both neurons and astrocytes throughout the brain,[17] with variations in glial or neuronal tropism of the vectors varying depending upon the brain region examined (Supplementary Figure 3). In the hippocampus, AAV9-2YF gave rise to high levels of expression in pyramidal neurons in the CA 1, 2 and 3, in the fimbria (Figures 4i and j) as well as numerous granule cells in the dentate gyrus, alongside astrocytes. We made similar observations for AAV9, with the exception of observing fewer GFP-expressing astrocytes and fewer granular cells in this region. In the striatum, with AAV9-2YF we observe expression in what appears to be medium spiny neurons as well as interneurons and astrocytes, whereas with AAV9 we observe sparse and faint GFP expression in neurons with only a few transduced astrocytes. In the cortex, AAV9-2YF leads to expression in pyramidal neurons in all

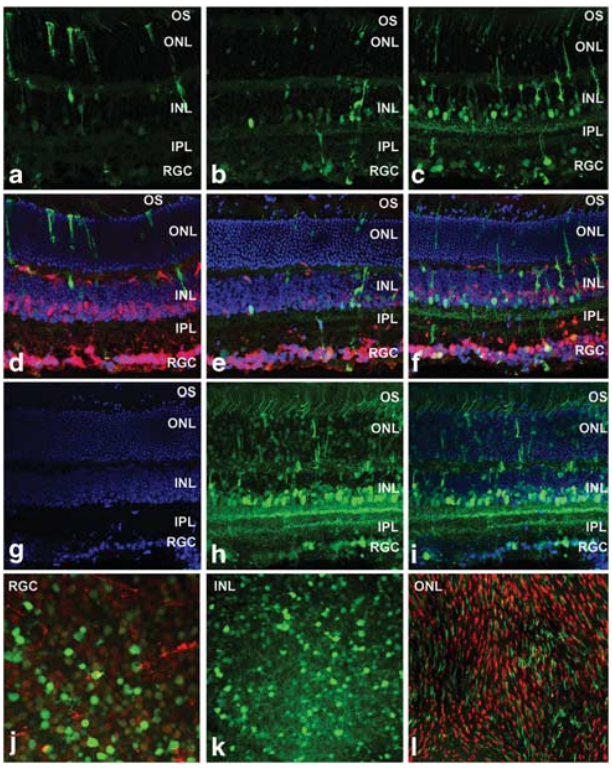

Figure 3 Detailed examination of retinal expression patterns using AAV9, AAV9-1YF and AAV9-2YF on transverse retinal sections. GFP fluorescence is shown for transverse retinal sections from 15 μm thick cryosections of eyes injected with (**a**) AAV9, (**b**) AAV9-1YF and (**c**) AAV9-2YF without anti-GFP immunostaining. The second row (**d–f**) shows the same images as (**a–c**) overlaid with 46-diamidino-2-phenyl indole (DAPI; blue) and NeuN (red) staining. The third row (**g–i**) shows a z-projection of a 15-μm thick retinal cryosection depicting expression with AAV9-2YF amplified by anti-GFP immunostaining. (**g**) Shows DAPI staining in blue and (**h**) depicts GFP fluorescence after immunostaining. The GFP and DAPI images are merged in (**i**). (**j–l**) Show a flatmount of a retina treated with AAV9-2YF. (**j**) Neurons were stained with NeuN in red at the RGC layer and (**k**) inner nuclear layer. (**l**) Cone photoreceptor labeling with peanut agglutenin Alexa-594 conjugate in red.

cortical layers as well as some astrocytes. Similar expression patterns were observed with AAV9, although the extent and level of expression were lower in this region. Finally, in the cerebellum AAV9-2YF generated to pronounced labeling of Purkinje cells, granule cells and astrocytes, whereas AAV9 mediated lower expression in neurons. High level of GFP expression was also seen in the hypothalamus (data not shown). This advance has implications for AAV9-mediated central nervous system gene delivery, particularly for diseases such as spinal muscular atrophy.[18] The use of the double tyrosine mutant AAV9 in future work may enable a reduction in the number of viral particles required to achieve similar rescue effects. This may be advantageous in lowering the risks of immune response to the virus. In addition to these applications, this technology offers an alternative to traditional transgenesis for basic neuroscience research.

Strong photoreceptor-specific expression using AAV9-2YF with a rhodopsin promoter

In both clinical and experimental gene therapy applications using systemic delivery, it will likely be necessary to restrict transgene

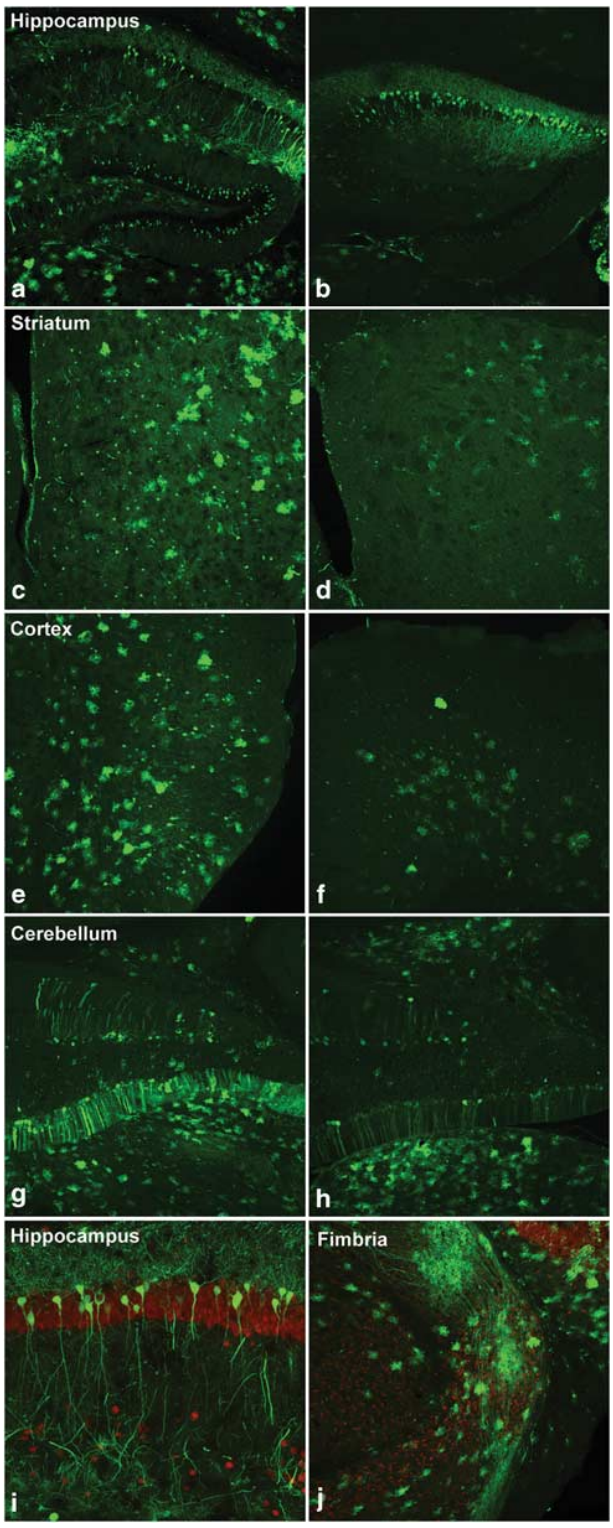

Figure 4 Brain sections illustrating GFP expression using AAV9-2YF vs AAV9. Representative fluorescence images of various brain regions showing GFP expression after transduction with AAV9-2YF (left column) vs AAV9 (right column). (**a, b**) Hippocampus, (**c, d**) striatum, (**e, f**) cortex and (**g, h**) cerebellum. The last row shows high magnification confocal images of AAV9-2YF-mediated GFP expression in the pyramidal cells in the CA1 of the hippocampus (**i**) as well as in the fimbria (**j**). Both sections were stained for NeuN to mark neurons (red).

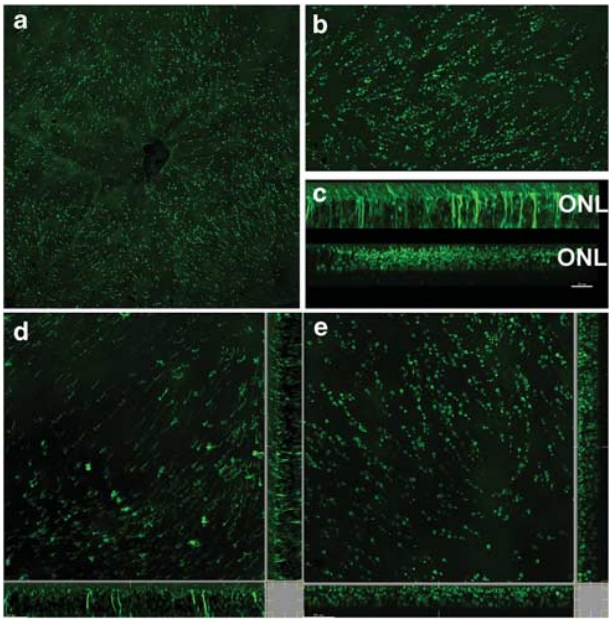

Figure 5 Expression patterns using AAV9-2YF-Rho-GFP (**a**) Confocal images of a retinal flatmount showing GFP expression after treatment with AAV9-2YF-Rho-GFP. Widespread expression can be observed around the optic nerve head (center), extending to the outer retina. (**b**) A z-projection of a zoom on the photoreceptor layer is shown from the contralateral eye mounted with the photoreceptor cells facing up. (**c**) Side views of 3D reconstructions from a retina showing GFP expression following AAV9-2YF-CAG-GFP administration (upper image) vs expression patterns mediated by AAV9-2YF-Rho-GFP (lower image), with the latter exhibiting restricted expression in the rod photoreceptors of the retina. (**d, e**) Oblique slice views of the 3D images in (**c**).

expression to a specific cell type. To this end, we replaced the ubiquitous CAG promoter used in the initial experiments with a mouse rhodopsin promoter and examined the expression patterns 3 weeks post injection. Our data show expression restricted to photoreceptor cells with no detectable expression in all other retinal cells (Figure 5) or in the brain (data not shown). This technology may thus be used to rapidly and economically generate somatic central nervous system transgenic animal models or gene knockdown animal models of photoreceptor diseases without costly and time intensive genetic manipulations. Most importantly, this approach offers the possibility of generating large animal models of diseases in which mutant proteins (that is, α-synuclein, P23H rhodopsin) that induce neurodegeneration can be expressed in the afflicted regions of the brain[24] or retina with AAV9-2YF-mediated transgenesis.

The clinical relevance of systemic gene delivery for treating retinal degenerations will more critically depend upon the ability to restrict gene expression to the cell type(s) of interest, and this specificity may be achieved through the use of cell specific promoters—as demonstrated here—or via miRNA strategies.[25] One major obstacle to the application of this technology in a clinical context is likely the risks of immune response to the capsid, which may pose significant safety concerns relative to local injections within the highly compartmentalized and immune privileged eye.[15] Regardless, the systemic injection of AAV is likely to be useful in the development of experimental gene therapies for inherited retinal degeneration, as many animal models of retinal degeneration follow a rapid progression compared with the human disease. We have observed significant levels of gene expression in retinal flatmounts from neonatal mice injected with AAV9-2YF 1 week post injection and steady levels of gene expression by the second week after the injection. This time course should enable gene replacement therapies before significant loss of photoreceptors and remodeling of the retina occurs in rodent models of blindness.

MATERIALS AND METHODS

Generation of recombinant AAV vectors

AAV vectors were produced by the plasmid co-transfection method.[26] Recombinant AAV was purified via iodixanol gradient ultracentrifugation as described previously[7] and titered by quantitative PCR relative to standards. Each vector contained a self-complimentary genome encoding GFP under the control of a ubiquitous CAG promoter or a single-stranded genome with GFP under the control of mouse rhodopsin promoter.

Intravascular injections

C57/BL/6 littermates were used for all studies. The postnatal day-1 pups were immobilized, and an operating microscope was used to visualize the tail vain. A total of 4×10^{11} Dnase-resistant particles of AAV9-scCAG-GFP, AAV9-1YF-scCAG-GFP, AAV9-2YF-scCAG-GFP or AAV9-2YF-Rho-GFP were injected in 10 µl volume. A correct injection was verified by noting blanching of the vein. After the injection, pups were allowed to recover for several minutes on a 37°C heating pad before being returned to their cages.

RT-PCR

Animals were humanely euthanized, and one retina was collected from n=5 (AAV9), n=4 (AAV9-1YF) or n=5 (AAV9-2YF) mice. RNA was extracted and subjected to DNase digestion, and the resulting RNA was used to create cDNA. RT-PCR for GFP, as well as the housekeeping gene glyceraldehyde-3-phosphate dehydrogenase as an internal control, was performed on samples in triplicate using validated primers. The ddCT method was used to calculate fold difference of GFP expression normalized to AAV9. An uninjected wild-type mouse retina served as a negative control.

Fundus photography

Fundus imaging was performed 2–8 weeks after injection (Micron II; Phoenix Research Labs Inc., Pleasanton, CA, USA). Pupils were dilated for fundus imaging with phenylephrine (2.5%) and atropine sulfate (1%).

Flatmounts

Retinal flatmounts were prepared by detaching the retina from the RPE. Radial cuts were introduced to flatten the tissue. The retinas were positioned with either the RGC or the photoreceptor side up to allow confocal imaging from both directions.

Peanut agglutinin labeling

Fixed retinas were rinsed 3× in phosphate-buffered saline before blocking and labeling with peanut agglutinin conjugated to Alexa-594 (1:40, Invitrogen, Carlsbad, CA, USA; Molecular Probes, Carlsbad, CA, USA) for 1 h. After rinsing, relief cuts were introduced and retinas were mounted for imaging.

Cryosections

Eyes were enucleated and immersion fixed in 10% formalin. The cornea and lens were removed, and the resulting eye-cups were cryoprotected in 30% sucrose before embedding in optimal cutting temperature medium for cutting.

Immunolabeling

Retinal cryosections were blocked in 1% bovine serum albumin, 0.5% Triton X-100 and 2% normal donkey serum for 2–3 h and treated with a rabbit anti-GFP monoclonal antibody at 1:500 (Invitrogen) and/or mouse anti-NeuN (MAB377, Chemicon, Billerica, MA, USA) in blocking solution overnight at 4 °C. After three phosphate-buffered saline washes, Alexa-488-conjugated anti-rabbit secondary antibody (Invitrogen) was applied at a 1:1000 dilution in blocking solution for 2 h at room temperature. The results were examined by confocal microscopy (LSM5; Carl Zeiss Microimaging, Peabody, MA, USA).

CONFLICT OF INTEREST

The authors declare no conflict of interest.

ACKNOWLEDGEMENTS

We thank Ryan Klimczak for performing the site-directed mutagenesis to generate the AAV9 single and double tyrosine mutants. We also thank Dr Alberto Auricchio for sharing the AAV-rho-GFP plasmid. This work was supported by grants from the NIH Nanomedicine Development Center for the Optical Control of Biological Function (PN2EY018241), the Foundation Fighting Blindness USA and the NIH grant RC2NS069476.

1 Cideciyan AV, Aleman TS, Boye SL, Schwartz SB, Kaushal S, Roman AJ *et al.* Human gene therapy for RPE65 isomerase deficiency activates the retinoid cycle of vision but with slow rod kinetics. *Proc Natl Acad Sci USA* 2008; **105**: 15112–15117.
2 Maguire AM, Simonelli F, Pierce EA, Pugh Jr EN, Mingozzi F, Bennicelli J *et al.* Safety and efficacy of gene transfer for Leber's congenital amaurosis. *N Engl J Med* 2008; **358**: 2240–2248.
3 Bainbridge JW, Ali RR. Success in sight: the eyes have it! Ocular gene therapy trials for LCA look promising. *Gene Therapy* 2008; **15**: 1191–1192.
4 Léveillard T, Sahel J-A. Rod-derived cone viability factor for treating blinding diseases: from clinic to redox signaling. *Science Trans Med* 2010; **2**: 26ps16.
5 Pang JJ, Dai X, Boye SE, Barone I, Boye SL, Mao S *et al.* Long-term retinal function and structure rescue using capsid mutant AAV8 Vector in the rd10 mouse, a model of recessive retinitis pigmentosa. *Mol Ther* 2009; **19**: 232–242.
6 Sanftner L. Glial cell line derived neurotrophic factor delays photoreceptor degeneration in a transgenic rat model of retinitis pigmentosa. *Mol Ther* 2001; **4**: 622–629.
7 Dalkara D, Kolstad KD, Caporale N, Visel M, Klimczak RR, Schaffer DV *et al.* Inner limiting membrane barriers to AAV-mediated retinal transduction from the vitreous. *Mol Ther* 2009; **17**: 2096–2102.
8 Kolstad KD, Dalkara D, Guerin K, Visel M, Hoffmann N, Schaffer DV *et al.* Changes in adeno-associated virus-mediated gene delivery in retinal degeneration. *Hum Gene Ther* 2010; **21**: 571–578.
9 Petrs-Silva H, Dinculescu A, Li Q, Deng W-T, Pang J-j, Min S-H *et al.* Novel properties of tyrosine-mutant AAV2 vectors in the mouse retina. *Mol Ther* 2009; **19**: 293–301.
10 Petrs-Silva H, Dinculescu A, Li Q, Min S-H, Chiodo V, Pang J-j *et al.* High-efficiency transduction of the mouse retina by tyrosine-mutant AAV serotype vectors. *Mol Ther* 2009; **17**: 463–471.
11 Klimczak RR, Koerber JT, Dalkara D, Flannery JG, Schaffer DV. A novel adeno-associated viral variant for efficient and selective intravitreal transduction of rat Müller cells. *PloS One* 2009; **4**: e7467.
12 Koerber JT, Klimczak R, Jang J-H, Dalkara D, Flannery JG, Schaffer DV. Molecular evolution of adeno-associated virus for enhanced glial gene delivery. *Mol Ther* 2009; **17**: 2088–2095.
13 Yin L, Greenberg K, Hunter JJ, Dalkara D, Kolstad KD, Masella BD *et al.* Intravitreal injection of AAV2 transduces macaque inner retina. *IOVS* 2011; **52**: 2775–2783.
14 Masland RH. The fundamental plan of the retina. *Nat Neurosci* 2001; **4**: 877–886.
15 Mingozzi F, High KA. Immune responses to AAV in clinical trials. *Curr Gene Ther* 2011; **11**: 321–330.
16 Bostick B, Ghosh A, Yue Y, Long C, Duan D. Systemic AAV-9 transduction in mice is influenced by animal age but not by the route of administration. *Gene Therapy* 2007; **14**: 1605–1609.
17 Foust KD, Nurre E, Montgomery CL, Hernandez A, Chan CM, Kaspar BK. Intravascular AAV9 preferentially targets neonatal neurons and adult astrocytes. *Nat Biotechnol* 2008; **27**: 59–65.
18 Foust KD, Wang X, McGovern VL, Braun L, Bevan AK, Haidet AM *et al.* Rescue of the spinal muscular atrophy phenotype in a mouse model by early postnatal delivery of SMN. *Nat Biotechnol* 2010; **28**: 271–274.
19 Zhang H, Yang B, Mu X, Ahmed SS, Su Q, He R *et al.* Several rAAV vectors efficiently cross the blood–brain barrier and transduce neurons and astrocytes in the neonatal mouse central nervous system. *Mol Ther* 2009; **19**: 1440–1448.
20 Rahim AA, Wong AM, Hoefer K, Buckley SM, Mattar CN, Cheng SH *et al.* Intravenous administration of AAV2/9 to the fetal and neonatal mouse leads to differential targeting of CNS cell types and extensive transduction of the nervous system. *FASEB J* 2011; **25**: 3505–3518.
21 Wu Z, Asokan A, Samulski RJ. Adeno-associated virus serotypes: vector toolkit for human gene therapy. *Mol Ther* 2006; **14**: 316–327.
22 Zhong L, Li B, Mah CS, Govindasamy L, Agbandje-McKenna M, Cooper M *et al.* Next generation of adeno-associated virus 2 vectors: point mutations in tyrosines lead to high-efficiency transduction at lower doses. *Proc Natl Acad Sci USA* 2008; **105**: 7827–7832.
23 Maingay M, Romero-Ramos M. Viral vector mediated overexpression of human alpha-synuclein in the nigrostriatal dopaminergic neurons: a new model for Parkinson's disease. *CNS Spectr* 2005; **10**: 235–244.
24 Ulusoy A, Decressac M, Kirik D, Bjorklund A. Viral vector-mediated overexpression of alpha-synuclein as a progressive model of Parkinson's disease. *Prog Brain Res* 2010; **184**: 89–111.
25 Ma C, Liu Y, He L. MicroRNAs–powerful repression comes from small RNAs. *Science China C Life Sci* 2009; **52**: 323–330.
26 Grieger JC, Choi VW, Samulski RJ. Production and characterization of adeno-associated viral vectors. *Nat Protoc* 2006; **1**: 1412–1428.

Supplementary Information accompanies the paper on Gene Therapy website (http://www.nature.com/gt)